J. Plasma Physics (1985), *vol.* 33, *part* 3, *pp.* 425–436
Printed in Great Britain

Plasmoid motion across a tangential discontinuity (with application to the magnetopause)

By J. LEMAIRE

Institut d'Aéronomie Spatiale de Belgique, 3 avenue Circulaire, B-1180 Brussels, Belgium

(Received 3 August 1984 and in revised form 14 December 1984)

The motion of a plasmoid (plasma-field entity) across an inhomogeneous magnetic field distribution of which the direction and strength change along the penetration trajectory has been studied. The bulk velocity decreases when the plasma element penetrates into a region of increasing magnetic field. The critical magnetic field intensity where a plasmoid is stopped or deflected is found to be the same critical field as that which has been observed in laboratory experiments for a non-rotating **B**-field distribution. The polarization electric field induced inside a moving plasma element has been determined for both low-β and high-β plasmoids. The momentum density vector of a plasmoid is deflected in the $-\mathbf{B}\times\nabla\mathbf{B}$ and $-\mathbf{B}\times(\mathbf{B}.\nabla)\mathbf{B}$ directions as it penetrates into an inhomogeneous **B**-field distribution. This kinetic model has been applied to the impulsive penetration of solar wind plasma irregularities impinging on the earth's geomagnetic field with an excess momentum density. As a consequence of impulsive penetration, a plasma boundary layer is formed where the intruding plasmoids are deflected eastward. Magnetospheric plasma is dragged in the direction parallel to the flanks of the average magnetopause surface. Diamagnetic effects of these impulsively penetrating plasmoids into the magnetosphere are also briefly discussed.

1. Introduction

Baker & Hamel (1965) have demonstrated experimentally that slightly diamagnetic plasma streams, injected into a region of uniform magnetic field, drift across the magnetic field lines with constant bulk velocity $\mathbf{v}_0$ when the integrated Pedersen conductivity of these field lines is zero or small: i.e. $\Sigma_p = \int \sigma_p dh \simeq 0$. This condition implies that the transverse Pedersen conductivity is small everywhere along the magnetic field line; i.e. not only in the collisionless plasma itself, but also in the walls of the vacuum tank through which the magnetic field lines pass.

Since, in these experiments, no external electric field ($\mathbf{E}_e$) is applied perpendicular to **B**, the single-particle kinetic approach as well as MHD theory would predict zero $\mathbf{E}\times\mathbf{B}$ drift velocities. Nevertheless, despite the absence of such an external **E**-field, plasma beams of finite widths in the $\mathbf{v}_0\times\mathbf{B}$ direction or injected plasmoids (i.e. plasma–magnetic field entities according to the definition of

Bostick (1956)) drift straight across the strong magnetic field and conserve their initial forward momentum, when $\Sigma_p = 0$. This indicates that the motion of plasmoids in an external magnetic field differs drastically from the motion of a single (test) particle in the same **B**-field distribution.

The reason for this difference has been described by Schmidt (1960). Indeed when n, the density of ions and electrons is great enough for the plasma dielectric constant ϵ to be much larger than unity, collective plasma effects lead to the accumulation of polarization charges which generates a local (internal) electric field, $\mathbf{E}_p$, inside the moving plasma element such that its initial momentum can be conserved.

Schmidt (1960) has described how the self-polarization $\mathbf{E}_p$ field builds up in a non-diamagnetic plasmoid injected into different magnetic field distributions of interest for laboratory experiments. Cross-field injection experiments can be divided into two categories: (i) wide plasma beams injected from plasma guns for which the beam width w is much larger than the ion gyroradius r_L^+, (ii) narrow high-energy neutralized ion beams injected from ion diodes and whose width is smaller than r_L^+. In the following we shall concentrate only on the first case which is relevant to a study of the interaction of the solar wind plasma stream with the earth's geomagnetic field. Indeed, for narrow energetic ion beams, the first-order guiding centre approximation, used below to calculate the ion and electron drift velocities averages over one gyromotion, fails to be applicable.

This study is also concentrated on cases where plasmoids are injected across an imposed external magnetic field distribution whose direction and intensity change as in a tangential discontinuity (see figure 1). This magnetic field topology simulates the magnetopause interface where the magnetic field direction changes from a northward direction in the magnetosphere to arbitrary orientations and intensities in the solar wind–magnetosheath region. Firstly, we have considered non-diamagnetic, low-β plasmoids. Next we discuss briefly the penetration of diamagnetic high-β plasmoids across a tangential discontinuity.

2. Non-diamagnetic plasmoids

Consider an external magnetic field like that illustrated in figure 1; the magnetic field direction has no component along the x direction and its B_y and B_z components are continuous functions of x. No externally imposed electric field is applied either parallel or perpendicular to **B**. A plasmoid is injected along the x axis with an initial velocity $\mathbf{v}_0$. The density inside the plasmoid is assumed to be large, so that the plasma dielectric constant is much larger than unity:

$$\epsilon = 1 + \frac{\frac{1}{2}nm^+c^2}{B^2/2\mu_0} = 1 + \left(\frac{\omega_p^+}{\Omega^+}\right)^2 \gg 1, \tag{1}$$

(ω_p^+ and Ω^+ are respectively the ion plasma frequency and Larmor gyrofrequency). This inequality is generally satisfied in laboratory plasma experiments, as well as in thermal space plasmas where $\epsilon = 10^3$–10^5. This implies that collective dielectric effects are important. Polarization charges build up a dielectric field in the plasma cloud and in its vicinity.

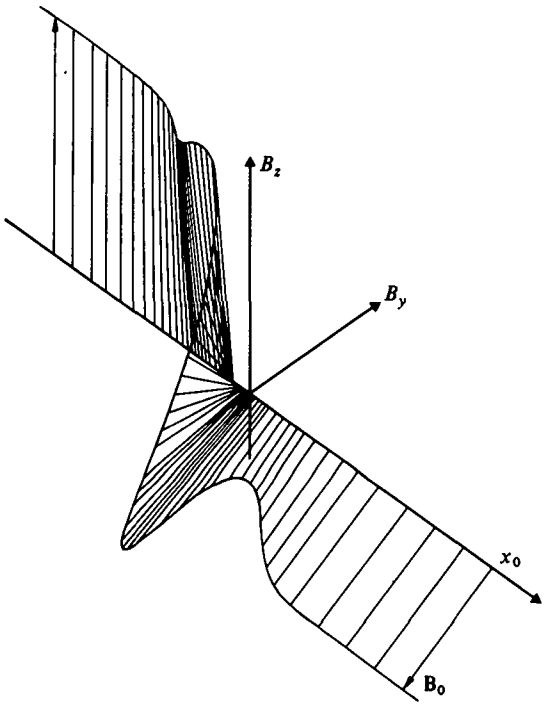

FIGURE 1. Rotating magnetic field distribution across a tangential discontinuity.

Furthermore, let us assume that the plasma density is small enough so that (i) the collision mean free path, l, of the electrons and ions is much larger than the dimensions of the system (i.e. the diameter of the vacuum tank or the density scale length in space plasmas), and also l is much larger than the corresponding Larmor gyroradius, r_L; (ii) the total kinetic energy density of the particles is much smaller than the magnetic energy density, i.e.

$$\beta = \frac{\frac{1}{2}nm^+v^2 + nk(T_\perp^+ + T_\perp^-)}{B^2/2\mu_0} \ll 1. \tag{2}$$

This latter condition implies that diamagnetic currents or other plasma currents produce additional magnetic fields which are small compared with the applied external magnetic field strength.

2.1. *Drift velocities*

Under these low-β conditions, the total **B**-field inside and outside the plasmoid is equal to the externally imposed field. When the variation of this field is small over a few Larmor gyroradii, the sum of all perpendicular drift velocity components can be determined from classical first-order orbit theory,

$$\mathbf{w} = \frac{\mathbf{E}\times\mathbf{B}}{B^2} + \frac{\mu}{qB^3}\mathbf{B}\times\nabla\left(\frac{B^2}{2}\right) + \frac{m}{qB^2}\mathbf{B}\times\frac{d\mathbf{w}_0}{dt}, \tag{3}$$

where the last two terms correspond respectively to the grad B drift and inertial

drift (Watson 1956; Longmire 1963); μ is the magnetic moment of a particle of mass m and electric charge q:

$$\mu = mV_\perp^2/2B. \tag{4}$$

We have assumed that the first-order guiding centre approximation is applicable and that μ is an adiabatic invariant. Note that this approximation breaks down for high-energy neutralized ion beams whose width is smaller than the ion Larmor gyroradius; it breaks also down in regions where the magnetic field strength becomes vanishingly small. The gyration energy of the particle around its guiding centre is $\frac{1}{2}mV_\perp^2$; $\mathbf{w}_0$ is the zeroth-order approximation of the guiding centre velocity:

$$\mathbf{w}_0 = V_\parallel \frac{\mathbf{B}}{B} + \frac{\mathbf{E}\times\mathbf{B}}{B^2} \tag{5}$$

By elimination of $\mathbf{w}_0$ in (3), the first-order approximation of the perpendicular component of the velocity of the guiding centre becomes

$$w_\perp = \frac{\mathbf{E}\times\mathbf{B}}{B^2} + \frac{\mu}{qB^2}\mathbf{B}\times\nabla B + \frac{mV_\parallel^2}{qB^4}\mathbf{B}\times(\mathbf{B}.\nabla)\,\mathbf{B} + \frac{m}{qB^2}\mathbf{B}\times\frac{d}{dt}\left(\frac{\mathbf{E}\times\mathbf{B}}{B^2}\right). \tag{6}$$

The last three terms in (6) are first-order corrections. They correspond respectively to the grad B, curvature and polarization drifts. Their directions are opposite for electrons ($q^- < 0$) and ions ($q^+ > 0$). These drifts are not necessarily small compared with the perpendicular component of the zeroth-order guiding centre velocity which, according to (5), is equal to

$$(\mathbf{w}_0)_\perp = \frac{\mathbf{E}\times\mathbf{B}}{B^2} \simeq \mathbf{v}. \tag{7}$$

For the magnetic field distribution illustrated in figure 1, $B_x = 0$ and the magnetic field lines are straight lines parallel to the (y, z) plane. Consequently $(\mathbf{B}.\nabla)\,\mathbf{B} = 0$, and the curvature drift is zero.

2.2. *Polarization electric field*

As a consequence of their oppositely directed drifts, the ions and electrons move perpendicular to **B** toward the lateral surfaces of the plasmoids where they accumulate (Schmidt 1960). Neglecting stray fields, and magnetization currents because of the low-β conditions, the rate of change of the electric field inside the moving element of plasma is given by

$$\frac{\partial\mathbf{E}}{\partial t} = -\frac{q^+n^+\overline{\mathbf{w}_\perp^+} + q^-n^-\overline{\mathbf{w}_\perp^-}}{\epsilon_0}. \tag{8}$$

For the sake of simplicity the electron and ion densities n^- and n^+ will be assumed equal and uniform inside the plasmoid.

After averaging the drift velocity over the velocity distribution of the ions and electrons, taking into account that $q^+n^+ = -q^-n^- = qn$, and neglecting the electron mass (m^-) as compared with the ion mass ($m^+ = m$), equation (8) becomes

$$\frac{\partial\mathbf{E}}{\partial t} = -\frac{nm}{\epsilon_0 B^2}\mathbf{B}\times\left[\frac{\overline{\mu^+} + \overline{\mu^-}}{m}\nabla B + \frac{d}{dt}\left(\frac{\mathbf{E}\times\mathbf{B}}{B^2}\right)\right]. \tag{9}$$

It can be seen from (9) that $\partial \mathbf{E}/\partial t$ is perpendicular to **B**. The polarization electric field building up with time is therefore also normal to **B**.

The factor $nm/\epsilon_0 B^2$ is equal to $\epsilon - 1$; since the plasma dielectric constant ϵ is very large, the value of the expression within the brackets in (9) must be very small in order to avoid unreasonably high values for $\partial E/\partial t$, the rate of change of the electric field intensity. Consequently,

$$\frac{d}{dt}\left(\frac{\mathbf{E}\times\mathbf{B}}{B^2}\right)+\frac{\overline{\mu^+}+\overline{\mu^-}}{m}\nabla B \simeq 0. \tag{10}$$

By combining (7) and (10), it can be deduced that $d\mathbf{v}/dt$ is a vector parallel to $-\nabla B$, i.e. parallel to the x axis.

$$\frac{dv}{dt} = v\frac{dv}{dx} = -\frac{\overline{\mu^+}+\overline{\mu^-}}{m}\frac{dB}{dx}. \tag{11}$$

Taking into account the adiabatic invariance of the magnetic moments μ^+ and μ^-, and integrating (11) from x_0 to x, we obtain

$$v^2(x) = v_0^2 + 2\frac{\overline{\mu^+}+\overline{\mu^-}}{m}[B_0 - B(x)]. \tag{12}$$

Using (4) and the definition of the perpendicular kinetic pressure

$$p_\perp = \tfrac{1}{2}nm\overline{V_\perp^2} = n\bar{\mu}B = nkT_\perp, \tag{13}$$

equation (12) becomes

$$\tfrac{1}{2}mv^2 + kT_\perp^+ + kT_\perp^- = \text{constant} = \tfrac{1}{2}mv_0^2 + (kT_\perp^+)_0 + (kT_\perp^-)_0. \tag{14}$$

This shows that the sum of the translational and the perpendicular thermal energy densities of the ions and electrons is a constant of motion. A similar result was derived by Schmidt (1960) for the two-stage plasma accelerator and non-rotating **B**-field distributions. Equation (12) has been verified experimentally by Demidenko *et al.* (1967, 1969) for plasmoids traversing inhomogeneous but non-rotating magnetic fields, and, whose intensity tended to zero for $x = \pm\infty$ (i.e. for $B_0 = 0$).

Note that when the magnetic field strength is independent of x (i.e. when $dB/dx = 0$) the bulk velocity of the plasmoid is constant and equal to v_0, even when the direction of **B** rotates as a function of x as illustrated in figure 1.

A plasmoid penetrating into a region of lower magnetic field intensity is accelerated by adiabatic diminution of the gyration energy (see (12) or (14)). In contrast, when a solar wind plasma element moves from the magnetosheath into the magnetosphere, where the **B**-field intensity is higher, it can be verified from (12) that the velocity of the intruding plasmoid decreases.

The components of the polarization electric field inside the plasmoid are given by

$$E_x(x) = v_z B_y - v_y B_z; \quad E_y(x) = v_x(x) B_z(x); \quad E_z(x) = -v_x(x) B_y(x). \tag{15}$$

When the magnetic field vector rotates, the polarization electric field (15) rotates by the same angle, but both field vectors remain orthogonal to each other; indeed it can be verified that $\mathbf{E}.\mathbf{B} = 0$ when $B_x = 0$.

2.3. *Non-uniform bulk velocities*

In the derivation of (8) and (9) a simple 'capacitor' model, first introduced by Schmidt (1960), has been used for the sake of simplicity. This model is based on the assumption that polarization charges 'accumulate' only at the surface of the plasmoid. This implies that the electron and ion densities are equal and uniform inside the whole plasma element. It was also assumed that these densities drop abruptly to zero outside the surface of the plasmoid. As a consequence of the polarization drift, grad B, and curvature drifts, the uniform electron and ion densities (n^- and n^+) are simply shifted in opposite directions. This produces surface polarization charges at the sharp boundaries of the plasmoid as in the case of a capacitor. But this shift of density distributions will not create a volume polarization density. Neglecting stray-fields near the edges, the resulting electric field inside an elongated plasmoid is then approximately uniform; the rate of variation of **E** can then also be derived from (8) or (9).

The 'water bag' or square distributions assumed for n^+ and n^- are, of course, ideal models; in reality, the plasma densities are more likely to be non-uniform. However, even for these less ideal, non-uniform density distributions, the oppositely directed drifts of electrons and ions give rise to surface polarization charges similar to those obtained with the uniform capacitor model, but in addition a non-zero polarization density is then created within the plasmoid. The resulting polarization electric field may therefore be non-uniform. As a consequence, the plasma can well have an internal non-uniform circulatory motion, in addition to the average forward velocity of its centre of mass.

When the plasma density is not uniform and when vortex or circulation flows exist inside a plasmoid, the equation of motion of the centre of mass must be considered instead of (12). The total mass and magnetic moment of the plasmoid enter in this equation of conservation of global momentum. But this would deserve a more detailed study not undertaken in this article.

2.4. *Critical magnetic field intensity*

From (12), a critical magnetic field strength B_1 can be deduced. Indeed, a plasmoid injected in a transverse magnetic field whose intensity increases steadily with x, will necessarily reach a position x_1 where its bulk velocity v has been reduced to zero. The plasma element cannot penetrate beyond this distance where the external magnetic field is equal to B_1:

$$B(x_1) = B_0 + \frac{mv_0^2}{2(\overline{\mu^+} + \overline{\mu^-})} = B_0\left[1 + \frac{mv_0^2}{m^+(\overline{V_\perp^+})_0^2 + m^-(\overline{V_\perp^-})_0^2}\right] \tag{16a}$$

or, equivalently,

$$B(x_1) = \frac{\frac{1}{2}mv_0^2 + (kT_\perp^+)_0 + (kT_\perp^-)_0}{\overline{\mu^+} + \overline{\mu^-}} \tag{16b}$$

from (14) and (13).

When the plasmoid reaches the point x_1, all the translational energy has been converted into perpendicular (gyration) thermal energy. Plasmoids are reflected adiabatically or dispersed transversely when they reach this point where the field strength is equal to B_1.

The critical magnetic field strength given by (16*b*) is the same as that deduced by Demidenko *et al.* (1969) for a non-rotating **B**-field distribution and for laboratory plasmas where the electron temperature (T^-) and magnetic moments (μ^-) were negligibly small. Note also that in these experiments the field B_0 at large distance is taken equal to zero.

At the distance of maximum penetration x_1, the y and z components of the electric field (15) both become equal to zero. Note however that $\mathbf{E}(x_1)$ can have a finite component in the x direction, i.e. perpendicular to the front edge of the plasmoid: $E_x(x_1) \neq 0$.

2.5. *Maximum penetration depth of solar wind plasmoids in the geomagnetic field*

A solar wind plasmoid penetrating impulsively in the magnetosphere traverses the magnetopause where the magnetic field generally has a zero or very small normal component ($B_x \simeq 0$). The magnetic field B_M inside the magnetosphere increases almost as R^{-3}, where R is the geocentric distance. As a consequence, there is always a penetration depth x_1 where $B_M(x)$ is equal to B_1, the critical magnetic field strength given by (16*a*) or (16*b*).

Let us now consider a plasmoid moving across the interplanetary magnetic field whose mean intensity is equal to $B_0 \simeq 6\,\mathrm{nT}$ (Ness, Hundhausen & Bame 1971; Hedgecock 1975); let the velocity of the plasmoid be $v_0 = 468\,\mathrm{km\,sec^{-1}}$, corresponding to the mean solar wind speed (Feldman *et al.* 1977), and let the electron and ion temperatures respectively be

$$(T^-)_0 = 1{\cdot}4 \times 10^5\,\mathrm{K} \quad \text{and} \quad (T^+)_0 = 1{\cdot}2 \times 10^5\,\mathrm{K};$$

it can then be verified from (16*a*) that $B_1 = B_0[1 + 2200/43] = 313\,\mathrm{nT}$. In the earth's dipole magnetic field B_M is equal to 313 nT at an equatorial distance $R_1 = 4{\cdot}6R_E$.

In the preceding numerical application, we have used the mean interplanetary magnetic field and solar wind parameters measured before the bow shock. However, through the bow shock the solar wind plasma parameters are drastically modified. When post-shock values are used, i.e.

$$B_0 = 30\,\mathrm{nT} \quad \text{and} \quad M_s^2 = mv_0^2/2k[T^+ + T^-] \simeq 0{\cdot}5$$

one obtains, from (16*a*), $B_1 = 45\,\mathrm{nT}$ and $R_1 = 8{\cdot}8R_E$ which is almost equal to the observed mean radial distance of the magnetopause at the subsolar point.

When M_s, the sonic Mach number, and/or when B_0, the magnetic field in the magnetosheath, increase, it can be verified from (16*a*) that B_1 increases also, and consequently that the radial distance of the average magnetopause position is pushed closer to the earth. Furthermore, from the first-order theory presented above, the penetration depth x_1 does not depend on the angle of rotation of the magnetic field across the magnetopause.

Magnetopause observations analysed by Fairfield (1971) and Formisano, Domingo & Wenzel (1979) confirm these theoretical results concerning (i) the average subsolar position of the earth's magnetopause, and (ii) its dependence on the solar wind bulk velocity. The observations support our theoretical conclusion

that (iii) the average magnetopause position does not significantly depend on the orientation of the interplanetary magnetic field. The dependence of the magnetopause position on the value of B_0, the interplanetary magnetic field strength, has not yet been checked statistically, at least to our knowledge.

It might be interesting to check whether these theoretical results will be confirmed by observations of Jupiter's and Saturn's magnetopause crossings when a significantly large number of them are available.

2.6. *Momentum density*

The momentum density in the plasmoid can be obtained from (3) or (6) by averaging $\mathbf{w}_\perp^+$ and $\mathbf{w}_\perp^-$ over the velocity distribution of the ions and electrons. At zeroth-order approximation, $\rho\mathbf{v} = \rho\mathbf{E}\times\mathbf{B}/B^2$, where $\rho = \Sigma n_i m_i$; at the first-order approximation and for a multicomponent plasma,

$$\rho\mathbf{v} = \sum_i n_i m_i \overline{\mathbf{w}_{\perp i}} = \rho\frac{\mathbf{E}\times\mathbf{B}}{B^2} + \sum_i \frac{[n_i m_i^2 \overline{V_{\perp i}^2}]}{2q_i}\frac{\mathbf{B}\times\nabla B}{B^3} + \sum_i \frac{[n_i m_i^2 \overline{V_{\parallel i}^2}]}{q_i}\frac{\mathbf{B}\times(\mathbf{B}.\nabla)\,\mathbf{B}}{B^4} + \sum_i \frac{n_i m_i^2}{q_i}\frac{\mathbf{B}}{B^2}\times\frac{d}{dt}\left(\frac{\mathbf{E}\times\mathbf{B}}{B^2}\right). \tag{17}$$

Note that $p_{\perp i}$ and $p_{\parallel i}$, the perpendicular and parallel components of the partial kinetic pressure for the ith particle species can be used to express the terms in the brackets of (17) by using (13) and

$$n_i m_i \overline{V_{\parallel i}^2} = n_i kT_{\parallel i} = p_{\parallel i}. \tag{18}$$

The third term on the right-hand side of (17) comes from the polarization drift and can be transformed by using (10) or

$$\frac{d}{dt}\left(\frac{\mathbf{E}\times\mathbf{B}}{B^2}\right) = -\frac{\Sigma_i n_i m_i \overline{V_{\perp i}^2}}{2\rho B}\nabla B - \frac{\Sigma_i n_i m_i \overline{V_{\parallel i}^2}}{\rho B^2}(\mathbf{B}.\nabla)\,\mathbf{B}. \tag{19}$$

Note that (19) is derived, as in § 2.2, for a uniform density distribution inside the plasmoid by taking into account that $\epsilon \gg 1$. It is applicable to general magnetic field distributions with curved field lines and for arbitrary values of β. Curvature currents must then, however, be considered, unlike in (10) where it is assumed that $(\mathbf{B}.\nabla)\,\mathbf{B} = 0$. It should also be pointed out that magnetization currents resulting from the circular motion of ions and electrons about their individual guiding centres do not contribute to a net transport of electric charges. Therefore these magnetization currents are not included in the right-hand side of (8).

When all terms of the order of m^-/m^+ are neglected in the first-order approximation, the momentum density for a two-component neutral plasma becomes

$$\rho\mathbf{v} = \rho\frac{\mathbf{E}\times\mathbf{B}}{B^2} - \frac{\rho}{q^+}\left[\frac{m^-}{2}\overline{(V_\perp^-)^2}\right]\frac{\mathbf{B}\times\nabla B}{B^3} - \frac{\rho}{q^+}[m^-\overline{(V_\parallel^-)^2}]\frac{\mathbf{B}\times(\mathbf{B}.\nabla)\,\mathbf{B}}{B^3}, \tag{20}$$

where the brackets can be expressed in terms of the perpendicular and parallel electron temperatures.

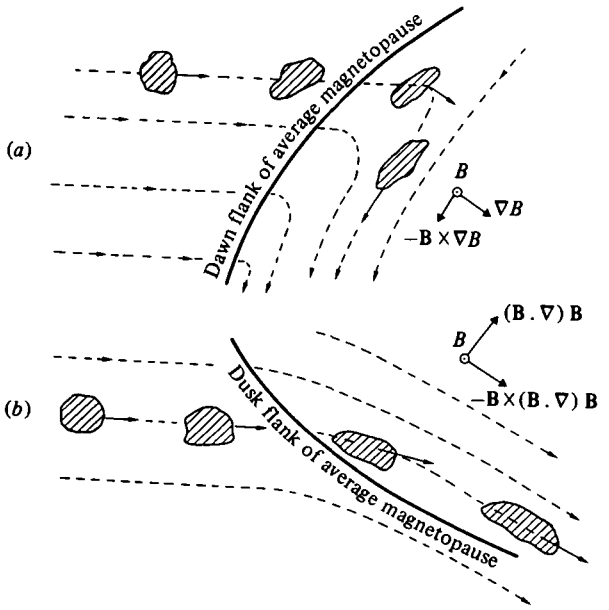

FIGURE 2. Eastward deflexion of solar wind plasmoids penetrating impulsively in the magnetospheric plasma boundary layer along (*a*) the dawn flanks and (*b*) dusk flanks of the magnetopause. Both the grad B and curvature drifts of the ions contribute to the eastward deflexion of intruding solar wind plasma irregularities.

These first-order correction terms are small when the electron temperature is small or when the gradient of B and the curvature of magnetic field lines are not large. Otherwise these corrections contribute to a deflexion of the plasmoid in the $-\mathbf{B}\times\nabla B$ and $-\mathbf{B}\times(\mathbf{B}.\nabla)\,\mathbf{B}$ directions, respectively.

2.7. *Viscous-like interaction*

It has been shown above that there is a critical magnetic field strength B_1 given by (16) where solar wind plasmoids are stopped or deflected. From (16) it can be seen that the penetration of plasmoids into the geomagnetic field is greatest when the interplanetary magnetic field strength, B_0, is greatest. Furthermore, it results also from this equation that larger values of B_1 are obtained for larger sonic Mach numbers. As a consequence, solar wind plasmoids with a flux of momentum density greater than the background will be stopped or deflected deeper into the geomagnetic field, i.e. beyond the mean position of the magnetopause where the condition $B_M = B_1$ is met for average solar wind plasma elements.

For a solar wind plasmoid impinging with an excess momentum on the geomagnetic field at the subsolar point or on the dusk flank as shown in the lower part of figure 2, the last two terms in (20) contribute to a deflexion toward dusk (i.e. eastward) in the 'plasma boundary layer'. Consequently, impulsive penetration of solar wind plasmoids into the plasma boundary layer transfers momentum to magnetospheric plasma along the flanks of the magnetopause. As a result of the electromagnetic coupling with the dayside cusp ionosphere via highly conducting geomagnetic field lines, this flux of momentum is also trans-

ferred to the ionosphere. These coupling and interaction processes correspond to 'viscous-like' interaction as suggested a long time ago by Axford & Hines (1961) and Hines (1964).

In the dusk flanks of the magnetopause region all three terms in (20) produce an eastward drag; in the dawn flanks the zeroth-order term (i.e. $\rho \mathbf{E} \times \mathbf{B}/B^2$) is initially predominant and contributes a westward (anti-sunward) drag. But deeper in the magnetosphere where the y and z components of the polarization electric field (15) become equal to zero in the vicinity of x_1, the first-order drift terms in (20) become the predominant ones. As a consequence, the flow direction changes from westward to eastward as illustrated in the upper part of figure 2. Orders of magnitude calculation indicate that the grad B drift velocity of a solar wind plasmoid penetrating through the magnetopause can range up to $1\,\mathrm{km\,sec^{-1}}$.

2.8. *Effects resulting from depolarization currents*

Up to this stage we have ignored the possibility that the polarization charges may be neutralized by transverse Pedersen currents flowing either within a collision dominated plasma, within conducting walls or in a resistive ionosphere.

This effect has already been discussed by several authors in the case of laboratory experiments (Bostick 1956; Baker & Hamel 1965; Schmidt 1960; Gol'ts & Khodzhaev 1969) as well as in the case of solar wind plasma irregularities penetrating into the magnetosphere (Lemaire 1977, 1983, 1985; Lemaire & Roth 1978). It has been suggested that solar wind plasmoids penetrating into the geomagnetic field transfer part of their excess of momentum to the ionosphere, and dissipate part of their excess energy by inelastic collisions and Joule heating in the ionosphere at dayside cusp latitudes. This non-adiabatic deceleration of impulsively injected solar wind plasmoids contributes to an additional and important term in the right-hand side of (19); in consequence, this short-circuiting effect enhances the polarization drift velocity in (17) (last term). It can be verified that this (non-adiabatic) deceleration contributes a significant additional transfer of momentum density to magnetospheric plasma in the boundary layer next to the magnetopause surface as well as to the dayside cusp ionospheric plasma. This additional drag is again eastward in the direction of the earth's rotation.

2.9. *Mass losses of plasmoids*

The question of mass loss of a dielectric plasmoid moving across transverse magnetic field lines, resulting from edge effects, electrostatic charge repulsion, of cross-**B** ion drift due to non-uniform or oscillating **E**-fields, has been considered in the literature by Dolique (1963), Schmidt (1960), Baker & Hamel (1965), Demidenko *et al.* (1966, 1967), Khizhnyak *et al.* (1969), Heikkila (1982). It will not be pursued here, although it deserves a more detailed study, which is outside the scope of this paper.

It should be emphasized, that mass losses of a plasmoid penetrating into the geomagnetic field, either by field-aligned expansion, or by particle trapping and precipitation in the dayside cusps upper atmosphere, are important physical

processes affecting solar wind plasma elements penetrating impulsively into the magnetosphere.

Impulsive precipitation in the dayside cusp ionosphere of magnetosheath ions and electrons along magnetic field lines extending to the frontside magnetopause region was observed for the first time by Carlson & Torbert (1980). The dissipation of energy of the precipitating particles in the atmosphere produces the well defined peak in the electron temperature up to an altitude of 1000 km at the latitude of the dayside cusps (Titheridge 1976).

A stationary kinetic model describing the flow of precipitation of magnetosheath injected ions and electrons through the topside ionospheric background plasma contained in a dayside cusp flux tube, has been described by Lemaire & Scherer (1978). Field-aligned currents and the formation of a double layer near 20000 km altitude were obtained in this kinetic model calculation. Although a time-dependent model would be preferable to simulate the expansion of solar wind plasmoids along geomagnetic field lines, the kinetic model of Lemaire & Scherer (1978) shows that double layers can form quite naturally at the interface between the warm magnetosheath plasma and the colder ionospheric plasma. Such field-aligned double layers or electrostatic shocks (possibly propagating downward) accelerate the precipitating electrons and produce upward streaming beams of cold ionospheric ions which penetrate in the intruding solar wind plasmoid and intermix there with the injected magnetosheath plasma.

3. Diamagnetic effects

Up to this stage the impulsive penetration has been discussed only for *non-diamagnetic* plasmoids which do not significantly perturb the externally applied magnetic field distribution. However, when the value of β is of the order of unity, as it is most of the time in the solar wind, large diamagnetic effects perturb the externally imposed geomagnetic field. This question has been discussed already in a recent article by Lemaire (1984).

It is important to recall, however, that, as a consequence of the penetration of diamagnetic plasmoids, the outer geomagnetic field distribution becomes distorted and variable in time. By vector superposition of the variable diamagnetic field carried by moving plasmoids and the main earth's magnetic field, one obtains patchy and time-dependent interconnexions of magnetic field lines as illustrated by Lemaire (1983). Along the bundles of geomagnetic field lines interconnected to those of interplanetary space in a dynamical way, energetic solar particles can be guided into the magnetosphere and precipitated in the polar caps. Conversely magnetospheric particles can sporadically pour out of the geomagnetic trap into the solar wind, as has been suggested by Lemaire (1977).

The typical flux transfer events (FTE) often observed in magnetograms near the magnetopause by Russell & Elphic (1979) and reported by many others, correspond to typical magnetic field signatures of high-β, diamagnetic plasmoids penetrating impulsively from the magnetosheath into the magnetosphere.

It is worth noting that (17) and (19) are valid for a diamagnetic plasmoid, but in the case of high-β plasmoids the magnetic field $\mathbf{B}$ is the sum of the externally

imposed **B**-field and the diamagnetic fields associated with all local and distant plasma currents. These electric currents have a magnetic dipole moment in addition to higher order multipole moments. The dipole–dipole interaction of two plasmoids, or of a diamagnetic plasmoid, with the earth's dipole magnetic field is another force which must be taken into account. But this is a separate topic which will be discussed elsewhere.

I have appreciated the help of staff members at the Institute for Space Aeronomy in Brussels. This work has been supported by the Ministère de l'Education Nationale and the Fonds National de la Recherche Scientifique. I wish also to thank C. M. Minnis for editing the manuscript.

REFERENCES

AXFORD, W. I. & HINES, C. O. 1961 *Can. J. Phys.* **39**, 1433.

BAKER, D. A. & HAMMEL, J. E. 1965 *Phys. Fluids*, **8**, 713.

BOSTICK, W. H. 1956 *Phys. Rev.* **104**, 292.

CARLSON, C. W. & TORBERT, R. B. 1980 *J. Geophys. Res.* **85**, 2903.

DEMIDENKO, I. I., LOMINO, N. S., PADALKA, V. G., RUTKEVICH, B. N. & SINEL'NIKOV, K. D. 1967 *Soviet Phys. Tech. Phys.* **11**, 1354.

DEMIDENKO, I. I., LOMINO, N. S., PADALKA, V. G., RUTKEVICH, B. N. & SINEL'NIKOV, K. D. 1969 *Soviet Phys. Tech. Phys.* **14**, 16.

DEMIDENKO, I. I., LOMINO, N. S., PADALKA, V. G., SAFRONOV, B. G. & SINEL'NIKOV, K. D. 1966 *Plasma Phys.* **8**, 433.

DOLIQUE, J. M. 1963 *Comptes-Rendus Acad. Sci. Paris*, **256**, 3984.

FAIRFIELD, D. H. 1971 *J. Geophys. Res.* **76**, 6700.

FELDMAN, W. C., ASBRIDGE, J. R., BAME, S. J. & GOSLING, J. T. 1977 *Solar Output and its Variations* (ed. O. R. White), p. 351. Colorado Associated University Press.

FORMISANO, V., DOMINGO, V. & WENZEL, K.-P. 1979 *Planet. Space Sci.* **27**, 1137.

GOL'TS, E. Ya. & KHODZHAEV, A. Z. 1969 *Soviet Phys. Tech. Phys.* **14**, 741.

HEDGECOCK, P. C. 1975 *Solar Phys.* **44**, 205.

HEIKKILA, W. J. 1982 *Geophys. Res. Lett.* **9**, 159.

HINES, C. O. 1964 *Space Sci. Rev.* **3**, 342.

KHIZHNYAK, N. A., DEMIDENKO, I. I., LOMINO, N. S. & PADALKA, V. G. 1969 *Soviet Phys. Tech. Phys.* **13**, 1022.

LEMAIRE, J. 1977 *Planet. Space Sci.* **25**, 887.

LEMAIRE, J. 1983 *A simulation of the interconnection between magnetic field lines and geomagnetic field lines* (available on video-cassette). IASB, Brussels.

LEMAIRE, J. 1985 *The Polar Cusp* (eds. J. Holtet and A. Egeland), 33-46. Reidel.

LEMAIRE, J. & ROTH, M. 1978 *J. Atmos. Terr. Phys.* **40**, 337.

LEMAIRE, J. & SCHERER, M. 1978 *J. Atmos. Terr. Phys.* **40**, 337.

LONGMIRE, C. L. 1963 *Elementary Plasma Physics*. Interscience.

NESS, N. F., HUNDHAUSEN, A. J. & BAME, S. J. 1971 *J. Geophys. Res.* **76**, 6643.

RUSSELL, C. T. & ELPHIC, R. C. 1979 *Geophys. Res. Lett.* **6**, 33.

SCHMIDT, G. 1960 *Phys. Fluids*, **3**, 961.

TITHERIDGE, J. E. 1976 *J. Geophys. Res.* **81**, 3221.

WATSON, K. M. 1956 *Phys. Rev.* **102**, 12.